Diffusion Dynamics of Hairy-Rod Polymers in Concentrated Solutions

G. Petekidis,* D. Vlassopoulos,* and G. Fytas

Foundation for Research and Technology−Hellas, Institute of Electronic Structure and Laser, P.O. Box 1527, 711 10 Heraklion, Crete, Greece

R. Rülkens and G. Wegner

Max-Planck Institut für Polymerforschung, P.O. Box 3148, 55021 Mainz, Germany

G. Fleischer

Fakultät für Physik und Geowissenschaften, Universität Leipzig, D-04103 Leipzig, Germany

Received March 23, 1998; Revised Manuscript Received June 29, 1998

ABSTRACT: Photon correlation spectroscopy was employed in the polarized geometry in order to investigate the dynamics of solutions of substituted poly(*p*-phenylenes) at high concentrations. The total concentration fluctuations were found to exhibit a two-step decay. The fast dominant relaxation was the classical cooperative diffusion, controlled by the osmotic pressure of the system, exhibiting a stronger concentration dependence compared to flexible polymers, and discussed in the framework of the wormlike model. On the other hand, the second diffusive process was not related to self-diffusion (as confirmed by independent pulsed field gradient NMR measurements) and could not be accounted for by the existing theories. The self-friction coefficient was found to exhibit a stronger concentration dependence than the cooperative friction coefficient. At high concentrations, a diffusive cluster process was detected, despite the high solubility of these polymers in different solvents. The characteristics of this mode depended strongly on the molecular weight.

I. Introduction

In the first paper of this series, referred to as part 1, the orientation dynamics of concentrated isotropic solutions of hairy-rod poly(*p*-phenylenes) with aromatic sulfonated side chains, termed PPPS, have been presented.[1] The pertinent findings discussed were shown to relate to the collective rotational motion of the Kuhn segments of the persistent semistiff chains and the cooperative motion of orientationally correlated segment pairs. Here, we present a detailed investigation of the intermediate scattering function of the same polymers in solution, to quantify the relaxation of concentration fluctuations in the concentrated isotropic regime. This study complements the previous one, and together they provide the necessary ingredients in order to understand the physics governing the solution dynamics and the interplay between orientation and concentration fluctuations in model semistiff hairy-rod type of polymers.

The dynamic structure factor is determined using dynamic light scattering in the polarized geometry, whereas additional information is provided from pulsed-field gradient (PFG) NMR data. As in the case of orientational fluctuations, this study presents a clear advantage over previous ones,[2,3] in that it provides truly molecular information (on concentration fluctuations) in the isotropic regime up to very high concentrations (about 60 wt %). Of the numerous investigations on the dynamics of concentration fluctuations in solutions of stiff polymers, most have focused on poly(γ-benzyl α-L-glutamate), PBLG.[4,5] Other polymers, which have been also studied in detail, include polyisocyanates[6] and biological molecules with high rigidity such as DNA[7] and rodlike colloids.[8] In all these studies more than one relaxation mechanism was observed in the polarized (VV) correlation function. Nevertheless, the origin of these processes is not yet fully established; the predictions of the mean-field theory of Doi, Shimada, and Okano (DSO)[9] for a bimodal correlation function near the nematic transition due to coupling of orientation with concentration fluctuations are partly confirmed only by one study of PBLG solutions.[5] Moreover, PBLG and other systems used so far,[5] although stiff due to their helical structure, do not possess strong inherent optical anisotropy to allow investigation of the orientational (VH) dynamics, thus rendering the interpretation of the VV dynamics ambiguous. This limitation has been overcome with the use of poly(*p*-phenylenes), which possess large optical anisotropy.[10] However, the investigation of the dynamics of these polymers was restricted to concentrations below 10 wt %, in the semidilute regime, due to dissolution problems,[2,3] and even in this regime, it was rather difficult to obtain truly molecular properties.

The concentration dependence of the cooperative diffusion coefficient, D_c, measured by dynamic light scattering depends on both thermodynamic and friction effects, and thus combined dynamic and static light scattering as well as self-diffusion or viscosity measurements are needed to interpret the data and understand the different contributions to the cooperative dynamics. In general, the experimental studies on stiff polymer solutions reveal distinct concentration dependence of D_c in comparison with flexible polymer chains.[3,5,7]

In this paper, we address the above-mentioned open questions related to the mechanisms of concentration fluctuations in the concentrated regime, by employing the poly(*p*-phenylenes) with aromatic sulfonated side groups, in combination with the information on orientation fluctuations, discussed in part 1.[1] The paper is organized as follows: Section II provides a concise review of the relevant theoretical approaches; section

S0024-9297(98)00451-3 CCC: $15.00 © 1998 American Chemical Society
Published on Web 08/21/1998

III contains the experimental information. The results are presented and discussed in section IV and the main conclusions are summarized in section V.

II. Theoretical Background

In general, the field correlation function $\langle E(q,t)E^*(q,0)\rangle \propto I_{VV}(q,t)$, deduced in a dynamic polarized light scattering experiment from the intensity correlation function through the Siegert relation (eq 8 of part 1), is of the form of eq 3 of part 1. In the scattering geometry, where the $x-y$ plane is the scattering plane and the scattered wavevector q is in the x axis, the polarized (VV) correlation function is related with the zz component $\alpha_{zz}(t)$ of the polarizability tensor, $\alpha(t)$. In the dilute region, photon correlation spectroscopy (PCS) probes single molecule dynamics; the correlation function for short ($qL < 1$), noninteracting polymer chains (with only the self-part ($P = Q$) surviving and l and m running over segments of the same chain) is a single-exponential decay function[11]

$$I_{VV}(q,t) = N\left[4\left(\frac{\partial n}{\partial c}\right)^2 n^2 + \frac{4}{45}\langle\gamma^2\rangle \exp(-6D_R t)\right]P(q,t) \quad (1)$$

where n is the refractive index of the solution and $(\partial n/\partial c)$ is the refractive index increment and $\langle\gamma^2\rangle$ is the mean square optical anisotropy of the polymer chain. In eq 1, where independent rotation from translation is assumed, $P(q,t)$ is the dynamic form factor, which for $qL < 1$ is dominated by the center of mass diffusion of the polymer chain ($P(q,t) \approx P(q) \exp(-q^2 D_0 t)$). For rigid rods, the translational diffusion coefficient as calculated by Broesma[12] is of the form

$$D_0 = D'[\ln(2L/b) - \gamma] \quad (2)$$

where $D' \equiv k_B T/6\pi\eta_s L$, with η_s being the solvent viscosity and γ a function of the aspect ratio that describes the corrections due to end effects. The dimensions of rodlike polymers in dilute solutions may be obtained by combining measurements of the rotational and the translational diffusion coefficients.[13] In the case of semistiff polymers, in addition to the above, the persistence length is also involved. Yamakawa and Fujii calculated[14] the translational diffusion coefficient of a wormlike chain with a persistence length l

$$D_0 = D' F(L/2l, b/2l) \quad (3)$$

Two different functional forms of F were given depending on whether the ratio L/l is larger or smaller than 4.56. Despite the low scattering intensity, which represents a problem for PCS measurements in the dilute regime (especially for longer rods), PCS remains a very powerful technique. It does not require any modification of the macromolecular structure (such as labeling for fluorescence studies) and also observes the equilibrium state (in contrast to relaxation techniques, such as electric birefringence).

The dynamics in the semidilute and concentrated region are largely affected by intermolecular interactions, which are negligible in the dilute region. Above the overlap concentration, c^*, concentration fluctuations relax through the cooperative diffusion mechanism. It is noted that for the case of semistiff polymers, the overlap number concentration ρ^* may be estimated from the average end-to-end distance L_e, assuming the rigid rod expression, $\rho^* = 1/L_e^3$ as discussed in part 1.[1] Cooperative diffusion is the relaxation mechanism for the concentration fluctuations in a nondilute solution, and thus the diffusion constant D_c is affected by both thermodynamic and friction effects according to[15]

$$D_c = (M/N_A)(1 - \upsilon\rho)(\partial\pi/\partial c)_{T,P}/f_c \quad (4)$$

where f_c is the cooperative friction coefficient, $(\partial\pi/\partial c)_{T,P}$ the osmotic modulus of the solution, and υ the monomer volume.

The first theory for the dynamics of nondilute rigid rod solutions was presented by Doi and Edwards (DE).[16] They used the tube concept to describe the dynamics of nondilute solutions of rods and assuming a free axial diffusion ($D_{||} = D_{||,0}$) and a frozen diffusion perpendicular to the rod axes ($D_\perp \approx 0$); they predicted that the translational diffusion of a rod decreases to half of its dilute value ($D_s = D_0/2$, using $D_{||,0} = 2D_\perp$) and it becomes concentration independent in the semidilute region. In this theory, the effects of finite diameter, molecular flexibility, and hydrodynamic interactions were not considered. The refinements of the DE theory concerning the self-diffusion relate to the introduction of finite thickness and flexibility. Edwards and Evans[17] used a mean-field theory to first calculate the slowing down of parallel diffusion. Later, Teraoka and Hayakawa[18] calculated the decrease of the perpendicular diffusion, whereas an extension of the Edwards−Evans model to a wider concentration range was achieved by Sato and Teramoto.[19] The average self-diffusion coefficient (using $D_{||,0} = 2D_{\perp,0}$) is then decreasing with ρ according to

$$D_s = \frac{D_0}{2}[(1 - aL^2 b\rho)^2 + (1 + \epsilon L^3\rho)^{-2}] \quad (5)$$

where α and ϵ are constants.

The flexibility can affect the dynamic behavior, and very often deviations between experiments and theory of rods are attributed to it.[4,5] Semiflexible polymer chains are usually described by the wormlike model.[14] The dynamics of such chains in nondilute solutions have been studied in the framework of two models: the reptation model for a wormlike chain[20] and the "fuzzy cylinder" model.[21] While the former predicts a concentration independent self-diffusion in the concentrated regime, the latter predicts a behavior similar to that of rodlike chains (eq 5) with renormalized dimensions L_e and b_e. In the "fuzzy cylinder" model,[21] the global motion of the chain can be identified with that of a segment distribution model with cylindrical symmetry. In a way, the motion of stiff chains can be described by a rod of an effective length L_e. The longitudinal diffusion is calculated by a mean-field Green function method and a hole theory; the basic assumption of the latter is that the longitudinal diffusion of the test chain occurs only when a "hole" that is larger than a critical size exists in the front of the test chain. Both methods give a similar $D_{||}$ for relatively low concentrations (semidilute region) whereas at high concentrations the hole theory can predict very sharp decrease of D_s with c,[20] in qualitative agreement with the cessation of translational diffusion predicted by Edwards and Evans.[17]

Concerning the effects of thermodynamics, several statistical mechanical theories have been used to calculate the osmotic modulus, $(\partial\pi/\partial c)_{T,P}$, for isotropic solutions of rodlike and stiff polymers and most of them differ in the prediction of the third virial coefficient, B_3.[21] Onsager's theory for rigid rods, which is also used in

the DSO framework,[9] calculated the osmotic pressure up to the second virial term and thus predicted a $(\partial\pi/\partial c)_{T,P}$ that scales linearly with ρ

$$(M/RT)(\partial\pi/\partial c)_{T,P} = 1 + 8\rho/\rho_n \quad (6)$$

where $\rho_n = 16/\pi bL^2$ is the Onsager prediction for the nematic transition in a solution of rodlike polymers. On the other hand, scaling particle theory[21] (SPT) (as other theories) calculates B_3 for both rodlike and wormlike spherocylinders, while B_2 retains the value of the Onsager's theory. Thus, an even stronger concentration dependence of $(\partial\pi/\partial c)_{T,P}$ is predicted[21]

$$(M/RT)(\partial\pi/\partial c)_{T,P} = [1 + B/(1 - v\rho) + 2C\rho^2/(1 - v\rho)^2]/(1 - v\rho)^2 \quad (7)$$

with $B = (\pi/2)(L^2b\rho + 6v)$, $C = (v + \pi b^3/12)[B - 2(v + \pi b^3/12)]$, and $v = (\pi/4)Lb^2 + (\pi/6)b^3$ the molecular volume of a spherocylinder. The deviation of SPT from Onsager predictions for the osmotic pressure is significant above a volume fraction $v\rho = 0.05$ (or above $\rho/\rho^{**} \approx 3$, with $\rho^{**} = 1/L^2b$), for a rod with aspect ratio $L/b = 50$.[21] Thus, in the concentrated regime the second virial approximation may underestimate the osmotic modulus.

Concerning the theoretical description of the dynamic structure factor measured by dynamic light scattering, the most complete approach so far for isotropic semidilute and concentrated solutions of rodlike molecules is the DSO theory,[9] which was subsequently reformulated by Maeda.[22] DSO first presented a general theory to calculate the static structure factor of concentrated solutions of rodlike polymers and then applied it to calculate the dynamic structure factor. These investigations take into account the rotation−translation coupling of the rod diffusion and various types of interactions, which cannot be neglected in nondilute systems, such as excluded volume interactions, entanglement effects, and hydrodynamic interaction, to calculate the intermediate scattering function $g(q,t)$. In the limit of low q values, $g(q,t)$ is described by a single exponential related with the cooperative diffusion coefficient. In addition to the initial decay rate, DSO predicts a double exponential for $g(q,t)$ near the isotropic to nematic transition. The fast mode becomes faster with concentration, while its amplitude increases, and the slow mode becomes weaker and slower. The two relaxation modes are diffusive and both describe the relaxation of the concentration fluctuations coupled to the orientation fluctuations; the coupling becomes more important as the system approaches the isotropic to nematic transition. However, there is not yet clear experimental confirmation of this prediction.

III. Experimental Section

Materials. We utilized the same PPPS samples listed in Table 1 of part 1.[1] Their enhanced solubility in the common organic solvents, allows the study of the diffusion and orientational (part 1) dynamics well into the concentrated region.

Photon Correlation Spectroscopy (PCS). We have recorded the autocorrelation function $G(q,t)$ of the polarized (VV) light scattering intensity $I_{VV}(q)$ with an ALV-5000/fast multi tau digital correlator using 320 channels, over the broad time range $10^{-7}-10^3$ s (see also part 1[1]). Both the incident laser beam and the scattered light were polarized vertically (V) with respect to the scattering plane. In the present experiment, the normalized correlation function $C(q,t) = \alpha g(q,t)$ obtained from the experimental $G(q,t)$ (eq 8 of part 1) is associated with the collective relaxation of the thermal concentration fluctuations of the system. In cases where more than one relaxation process contributes to the scattering intensity, the combined use of static and dynamic light scattering is proven a very powerfool tool enabling the separation of the intensity of the each process. The analysis of $C(q,t)$ proceeds via inverse Laplace transformation (ILT, eq 9 of part 1), which allows the determination of the relaxation rate Γ_i and intensity $I_i(=\alpha_i I)$ of the partitioning processes; I is the total light scattering intensity and α_i the amplitude of the process revealed by the distribution relaxation function $L(\ln \tau)$. To examine the extent of association[3] and discriminate between relaxation processes of molecular and supramolecular origin, we have investigated S3 in three common organic solvents (toluene, $CHCl_3$, and trichloroethylene (TCE)).

Pulsed Field Gradient NMR. This technique measures essentially a stimulated echo using a proton spin as a probe, yielding the self-diffusion coefficient, D_s, of particles bearing ^{1}H nuclei, if the field gradient is applied as a pulse during the spin−echo experiment.[23] A magnetic gradient pulse of magnitude g is applied for a dephasing period δ, and the echo amplitude $\Psi(q,t)$ is measured during the time interval t between the field gradient pulses. The longest accessible diffusion times are determined by the spin−lattice relaxation time T_1, which is of the order of seconds; t may be varied between 10^{-3} s and T_1.

Results and Discussion

In general, the dynamic behavior of the solutions, as revealed in the polarized correlation function, becomes more complicated as the concentration is increased. Thus whereas in the dilute or early semidilute regime only one relaxation process is observed and originates from the translational diffusion of the polymer chains, at higher concentrations at least two more modes evolve. The slow one becomes stronger and slower with increasing concentration, while being solvent dependent, and as such it is attributed to the formation of clusters. The main, fast mode, which is a continuation of the translational diffusion in the semidilute and concentrated regimes is attributed to the cooperative diffusion of the polymer chains. Finally, an intermediate relaxation process is resolved in the semidilute region with the characteristics of a second diffusive cooperative mode.

Figure 1 shows experimental $C(q,t)$ at 25 °C and $q = 0.035$ nm^{-1} ($\theta = 150°$) for S3 solutions in three solvents at comparable concentrations, together with the respective distributions of relaxation times. The rate and the intensity I (corrected for the difference in the refractive index increment dn/dc) of the cooperative diffusion process assume similar values in the solutions, whereas the intensity I_s of the slow process depends on the choice of the solvent; low and high I_s are reported for the toluene and TCE solutions, respectively. On the basis of this finding, we have mainly focused in PPPSs toluene solutions with the least tendency for association. From the five PPPS samples, only the shortest S10 displays significant contribution of the slow process to the experimental $C(q,t)$; even at the smaller concentrations ($c/c^* \approx 1$), S10 exhibits a slower than the cooperative diffusion mode, which is active in the VH scattering as well.[1]

A. Dilute Regime−Translational Diffusion. At dilute concentrations, $C(q,t)$ is a single decay process with a diffusive decay rate $\Gamma = D_0q^2$, where D_0 is the translational diffusion of the polymer chain. Moreover, in the limit $c \rightarrow 0$ (Figure 2 below), diffusion coefficients deduced from PCS as well as NMR measurements should reveal the translational diffusion coefficients of a single polymer chain. Poly(*p*-phenylenes) have been verified experimentally as semiflexible chains. A per-

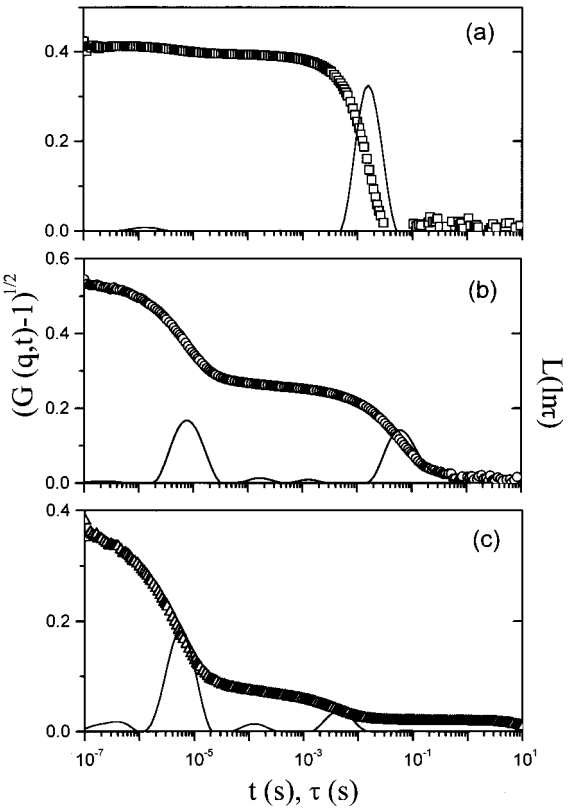

Figure 1. Experimental concentration correlation (field) functions at $q = 0.035$ nm^{-1} ($\theta = 150°$) and 25 °C for (a) S3 in TCE (73 mg/mL), (b) S3 in $CHCl_3$ (63 mg/mL), and (c) S7 in toluene (68 mg/mL). The corresponding distribution of relaxation times $L(\ln \tau)$ are also shown.

sistence length of the order of 25 nm was obtained by depolarized light scattering measurements[10] for PPPs with dodecyl flexible side chains. On the other hand, viscosimetry measurements[24] on the present PPPS give a significantly smaller value ($l = 13$ nm). A comparison of the two techniques[10,25] has shown that viscosimetry systematically yields lower l values than depolarized light scattering. Since all samples (except the smaller S10) used in these study have $L > l$, the theoretical expressions for semistiff chains must be used.

The dependence of D_0 on the contour length (L_w), the diameter (b), and persistence (l) length for a wormlike chain is described by eq 3. The theoretical predictions of the translational diffusion coefficients for rigid rods and semistiff chains agree with most experimental findings on various biological[7b,c] and synthetic[26] macromolecules. A compilation of the experimental and the calculated D_0 according to Broesma's expression (eq 2) and Yamakawa-Fujii (eq 3) for rigid and semiflexible chains, respectively, is presented in Table 1. In the computation we have used the characteristic lengths $b = 1.7$ nm and $l = 25$ nm (or $l = 13$ nm) and L_w values obtained from M_w of Table 1 of part 1.[1] For S1, S3, and S9, eq 3 with $l = 25$ nm describes very well the experimental D_0; for S7, eq 3 approximates the experimental D_0 with an error of 16%.

The dependence of the diffusion coefficient on the molecular weight ($D_0 \propto M^{-x}$) can provide information on the conformation of the polymer chain. In the presence of polydispersity the diffusion coefficient measured by PCS is the z-average. In the case of long rigid rods, $D_0 \propto L^{-1}$ (neglecting the logarithm and the end term correction of eq 2) and $(1/L)_z = 1/L_w$; hence we will

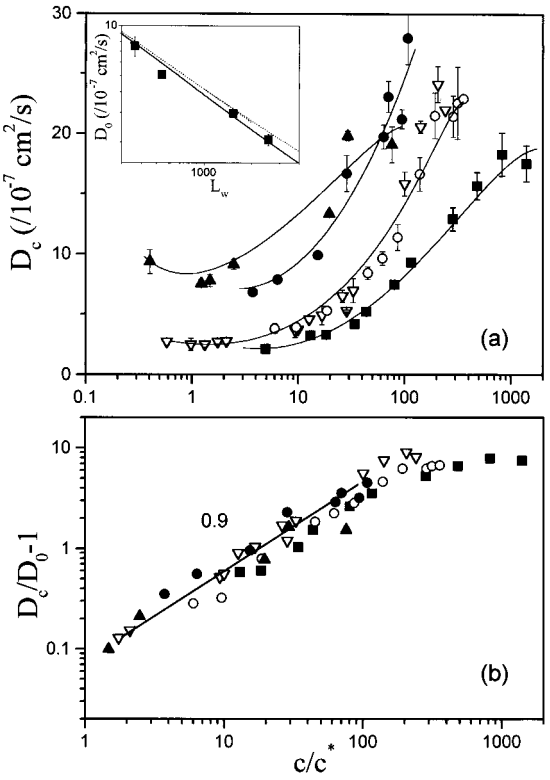

Figure 2. (a) Diffusion coefficient for the decay of the concentration fluctuations in PPPS solutions: S1 (■), S7 (●), S9 (▲) in toluene, S3 in chloroform (○) and TCE (▽). The dependence of the translational diffusion D_0 at c → 0 on the chain length is shown in the inset where the solid and dotted lines denote the prediction of eq 3 with $l = 25$ nm and $l = 13$ nm, respectively (see in text). (b) The dependence of the cooperative diffusion coefficient D_c (normalized with D_0) on the reduced concentration c/c^* for four PPP/S samples. The slope 0.9 represents an average fit to the experimental data.

Table 1. Dilute Solution Translational Diffusion Coefficients of PPPS[a]

sample	$D_{0,exp}$ (10^{-7} cm^2/s)	$D_{0,3}$ (10^{-7} cm^2 /s)	$D_{0,4a}$ (10^{-7} cm^2/s)	$D_{0,4b}$ (10^{-7} cm^2/s)
S1	2.06 ± 0.16	1.6	2.01	2.3
S3	2.97 ± 0.15	2.39	2.85	3.17
S7	5.06 ± 0.08	5.12	5.92	6.23
S9	7.53 ± 1	6.67	7.79	8.08

[a] $D_{0,exp}$, experimental zero concentration diffusion coefficients; $D_{0,3}$, theoretical value according to eq 3; $D_{0,4a}$, theoretical value according to eq 4 and $l = 25$ nm; $D_{0,4a}$, theoretical value according to eq 4 and $l = 13$ nm.

use M_w to determine the molecular weight dependence of D_0. The log−log plot of D_0 vs L_w shown in the inset of Figure 2 reveals behavior intermediate between flexible ($x = 0.5$ or 0.59) and rigid rod polymers; since $x = 0.63 \pm 0.04$. Although, higher x values (0.7−0.9) have been found in other solution studies of semistiff polymers,[26,27] we should note that this exponent is only indicative of the proximity to the rod or the coil limit in a rather limited range of molecular weights. It is clear that as the contour length increases many times above the persistence length, the apparent x will tend toward 0.59 for good solvents.

The comparison of the predictions of eq 3 for $l = 25$ nm (solid line) and $l = 13$ nm (dashed line) with experiment is depicted in the inset of Figure 2a. It is evident from Table 1 and Figure 2a that the experimental single chain translational diffusion supports a

persistence length $l = 25$ nm in agreement with the depolarized light scattering study[10] for the PPPs (with dodecyl side chains). This might suggest that the flexibility of the poly(*p*-phenylenes) with side chains is mainly determined by their backbone structure. Moreover, this consistent representation of D_0 for the four PPPS samples (M_w between 27 000 and 189 000) excludes molecular association and supports the validity of eq 3 for the present hairy-semistiff chains.

B. Semidilute−Concentrated Regime. With increasing concentration, chain interactions change the mechanism for the relaxation of the thermal concentration fluctuations. In the semidilute regime, cooperative rearrangements of the interacting chains are responsible for the temporal decay of the $g(q,t)$ with wavevector q. Hence, the cooperative diffusion, $D_c = \Gamma/q^2$, bears both kinetic and thermodynamic effects (eq 4). The friction increases with concentration due to interpenetration and noncrossability of polymer chains, while the thermodynamic interactions (under good solvent conditions) tend to speed up the cooperative diffusion. These two opposing forces are key issues in the investigation of polymer solutions and can be studied through the concentration dependence of the self-diffusion coefficient, D_s, and osmotic compressibility, $(\partial\pi/\propto c)_{P,T}$. The passage from the dilute to the semidilute regime should be marked by a change in both the dynamic and static quantities of the solution, i.e., the diffusion coefficient and the scattering intensity. A change in the behavior of D_c with concentration was observed by Tracy and Pecora[13] at about $10-20c^*$ for a PBLG solution, marking the passage to the semidilute region. A rather prolonged dilute solution behavior of the dynamic and static properties has been observed in most studies of stiff polymers,[3−5,13] revealing the more loose structure of stiff chains compared to their flexible counterparts, which allow for less intra- and weaker intermolecular interactions and, hence, easier interpenetration above c^*.

(i) Osmotic Compressibility. The osmotic modulus of the solution can be obtained from the light scattering experiment through the intensity of the scattered from isotropic concentration fluctuations light, according to

$$\frac{Kc}{R_{iso}} = \frac{(\partial\pi/\partial c)_{T,P}}{RT}(1 + \xi^2 q^2 + ...) \qquad (8)$$

with $K = 4\pi^2 n^2 (\mathrm{d}n/\mathrm{d}c)^2 \lambda^{-4} N_A^{-1}$, R_{iso} being the isotropic Rayleigh ratio, which is proportional to the scattered intensity, $I(q=0)$, and λ the wavelength of the incident radiation. From the measurements of the polarized correlation function one can deduce the contribution of the cooperative mode, responsible for the concentration fluctuations, according to $I_c = a_c I$. The extrapolation of I_c to the thermodynamic limit ($q = 0$) yields the osmotic compressibility $(\partial\pi/\partial c)_{P,T}$.

Estimation of $(\partial\pi/\partial c)_{P,T}$ from static light scattering measurements can often yield smaller values as compared to data from other more direct methods, such as membrane osmometry, especially at nondilute solutions due to the existence of aggregates or other relaxation processes besides the cooperative diffusion.[28] In these cases, utilization of the dynamic intensity of the cooperative process can provide better estimation of the osmotic modulus in semidilute polymer solutions. Experimental data for flexible chains[29] suggest that the osmotic modulus is independent of the molecular weight and can be fitted well by the expression predicted by

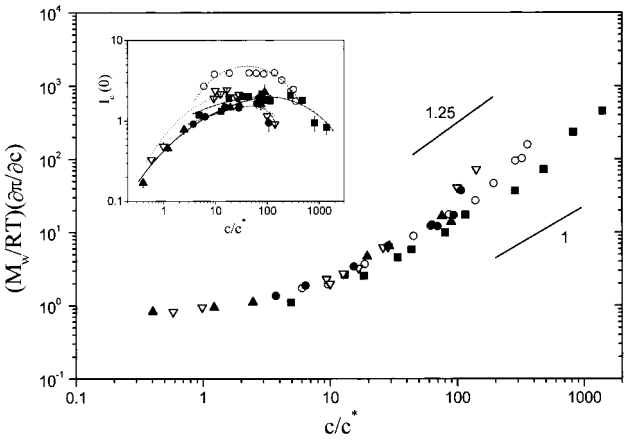

Figure 3. Concentration dependence of the osmotic modulus (normalized with molecular weight) as reduced from the cooperative intensities for solutions in toluene S1 (■), S7 (●), S9 (▲), and S3 in chloroform (○) and TCE (▽). The slopes denote scaling predictions for flexible (1.3) and rodlike (1) chain conformation. The concentration dependence of the normalized cooperative intensities $I_c(q = 0)$ for these samples are shown in the inset.

renormalization group theory[30] (RG). The RG expression, which is a function of $A_2 M_w c \sim c/c^*$, has a limiting behavior at high concentrations that agrees with the scaling prediction $c^{5/4}$.[15] On the other hand experimental studies of stiff chains in solution have shown that the increase of osmotic modulus is in general weaker, compared to solutions of flexible chains,[5,28,31] and thus it cannot be fitted by the RG theory.

The initial rate of increase of I_c with c decreases as the concentration exceeds c^*, and I_c displays a rather shallow maximum (inset of Figure 3) marking the passage to the semidilure regime which is characterized by the increased repulsion among polymer chains and thus suppression of concentration fluctuations. Figure 3 shows the normalized osmotic modulus $(M_w/RT)(\partial\pi/\partial c)_{P,T}$ versus c/c^* for four PPPS samples at 25 °C (in the dilute regime $(\partial\pi/\partial c)_{P,T} = RT/M$). In this reduced plot, the semidilute scaling prediction for flexible chains in good solvent, $(\partial\pi/\partial c)((c/c^*)^{5/4})$, is independent of chain length, while the Onsager mean field prediction for rigid rods (eq 6) $(\partial\pi/\partial c) \propto (b/L)(c/c^*)^1)$, depends on the aspect ratio. The experimental data fall between the mean field and the flexible scaling prediction, while at high concentrations they do not superimpose into a single curve. The poor superposition of the data in Figure 3 might reflect L dependence of the virial coefficients due to the variation of the rodlike character within these samples, i.e., different L/l ratios.

In Figure 4 we depict the osmotic compressibility data for different molecular weights and solvents as a function of polymer concentration (in weight percent) along with the theoretical predictions of the scaling particle theory, SPT (eq 7) (solid line), the Onsager mean-field theory (dotted line), and the renormalization group theory (dashed line). It can be seen that the SPT for wormlike spherocylinders can provide a good description of the experimental data. At the same time, the Onsager prediction exhibits a weaker increase of $(\partial\pi/\partial c)$ than experimentally observed at high concentrations, while the RG theory for flexible chains predicts higher $(\partial\pi/\partial c)$ at intermediate concentrations and does not conform to the observed increase at high concentrations since it reaches the scaling behavior ($c^{5/4}$) (Figure 4a). For all molecular weights in toluene, the data can be

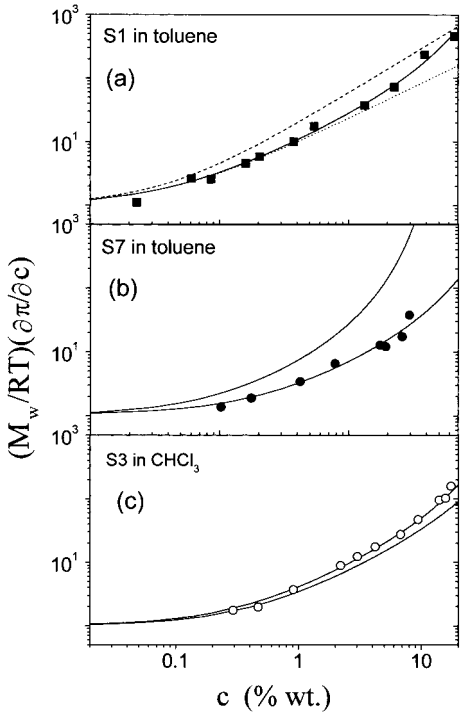

Figure 4. Experimental and theoretical concentration dependence of the normalized osmotic modulus for different M_w and solvents: (a) S1 in toluene (■), solid line, SPT theory (eq 7), $b = 0.8$ nm and L_w and M_w from Table 1 of part 1;[1] dotted line, Onsager theory (eq 6), $b = 0.8$ nm; dashed line, RG theory with $b = 0.8$ nm. (b) S7 in toluene (●); solid lines, SPT theory for $b = 0.8$ and 1.7 nm. (c) S3 in $CHCl_3$ (○), solid lines, SPT theory with $b = 1$ and 0.8 nm.

fitted very well by eq 7 using a diameter $b = 0.8$ nm,[10] whereas the curve corresponding to the fit of eq 7 with $b = 1.7$ nm is also shown for comparison in Figure 4b for S7 toluene solutions. This value is almost half the value used to describe the translational diffusion data (Figure 2a) representing the hydrodynamic diameter of the chain; the latter might be sensitive to the presence of long flexible side chains. From the osmotic compressibility data of PPPS in TCE and $CHCl_3$ the adjustable parameter b was found to be different; as for S3 in $CHCl_3$ we obtain the best fit using $b = 1$ nm (the corresponding to $b = 0.8$ nm curve according to eq 7 is also shown in Figure 4c). For S3 in TCE the best fit is otained by using $b = 1.3$ nm. It appears that the value of b deduced from the thermodynamic quantity $(\partial\pi/\partial c)$ reflects more the diameter of the chain backbone.

(ii) Cooperative Diffusion. The variation of D_c with concentration is visualized for four PPPS samples in Figure 2; the linear $D_c(c)$ at low concentrations allows the estimation of D_0 at $c \rightarrow 0$. To reveal the c dependence of D_c at higher concentrations, it is more appropriate to examine the reduced quantity $D_c/D_0 - 1$ implied by the general form

$$D_c = D_0 (1 + k_c c^{\nu}) \qquad (9)$$

where k_c and ν are material constants depending on the solvent quality. The phenomenological description of D_c by eq 9 may describe the behavior of the cooperative diffusion of semistiff and rodlike polymers. Nevertheless, a more rigorous analysis of data in an effort to check the theoretical predictions requires the separation of the frictional from the thermodymamic contribution

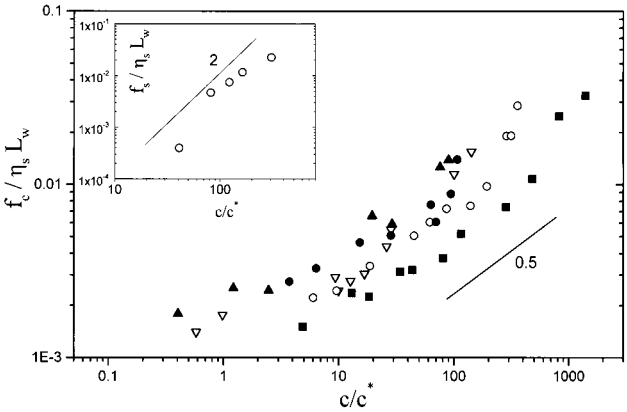

Figure 5. Normalized mutual friction coefficient (eq 4) in four PPPS samples as a function of the reduced concentration in three solvents: S1 (■), S7 (●), S9 (▲) in toluene, S3 in chloroform (○) and TCE (▽). Inset: Concentration dependence of the self-friction coefficient in S3/chloroform solutions from PFG-NMR data.

in D_c. In such a case, if for example eqs 4, 5 and 7 are combined, a complicated expression for the cooperative diffusion is obtained that is difficult to be verified using D_c data unless the thermodynamic or the frictional contribution can be accounted for. We have already confirmed the ability of the SPT to describe the thermodynamic behavior of solutions of the present stiff PPPSs. Next, it should be examined whether the friction coefficient involved in the cooperative diffusion (eq 4) represents the self-diffusion friction. The latter quantity is actually predicted by several theories which deal with the self-diffusion of wormlike or rodlike chains in solution as discussed in section II.

Self-diffusion data on synthetic stiff polymers are rather limited. Measurements were carried out with solutions of PBLG,[32] mainly by force Rayleigh scattering and indicated a decrease of the D_s with c. The work of Tinland et al.[33] with biological wormlike xanthan molecules is also worth noting; using several molecular weights they reported a sigmoidal-type curve of reduction of D_s with c, i.e., constant in the dilute, decreasing in the semidilute region, and leveling off in the concentrated region. More recently, Bu et al.[34] measured the self-diffusion of PBLG by fringe pattern recovery after photobleaching and again found two or three regimes depending on the molecular weight.

The cooperative friction f_c can be computed from eq 4 and compared with the self-diffusion D_s of the PFG-NMR experiment. The concentration dependence of these friction coefficients per unit length (corrected for the different solvent viscosities) is shown in Figure 5. As expected, both frictions increase with concentration, but unexpectedly f_c reveals a dependence on the chain length. S1 appears to display lower friction than the shorter S9 chain, which might be attributed to the larger dynamic flexibility of the former. Note that the orientational times at high concentrations are also faster in S1 than in S9 (Figure 8 of part 1). The self-friction for the S3 solutions in chloroform obtained from D_s shows stronger c dependence than f_c reflecting the different nature of these two physical quantities. The large disparity between f_c and f_s makes therefore any attempt to associate the composite cooperative diffusion with wormlike theories rather questionable (all models assume that cooperative and self-frictions are the same).

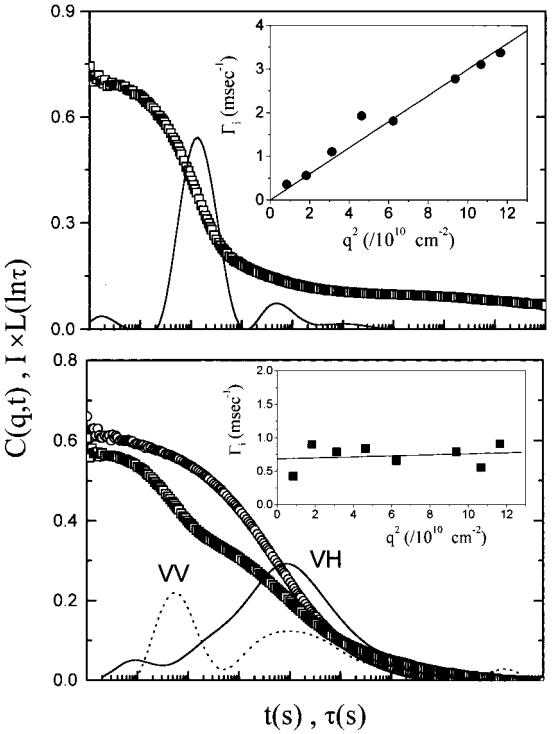

Figure 6. (a) Polarized field correlation function for S1 solution in toluene (115 mg/mL) at $q = 0.025$ nm^{-1} ($\theta = 90°$) along with the corresponding distribution $L(\ln \tau)$ (multiplied with the normalized intensity) and the diffusive rate of the intermediate mode (inset). (b) Polarized (VV) and depolarized (VH) field correlation functions for S1 solution in toluene (335 mg/mL) at $q = 0.034$ nm^{-1} ($\theta = 150°$) with the corresponding $L(\ln \tau)$ (multiplied with the normalized intensity). The variation of the rate Γ_i with q for the intermediate mode in the dynamic VV scattering is shown in the inset.

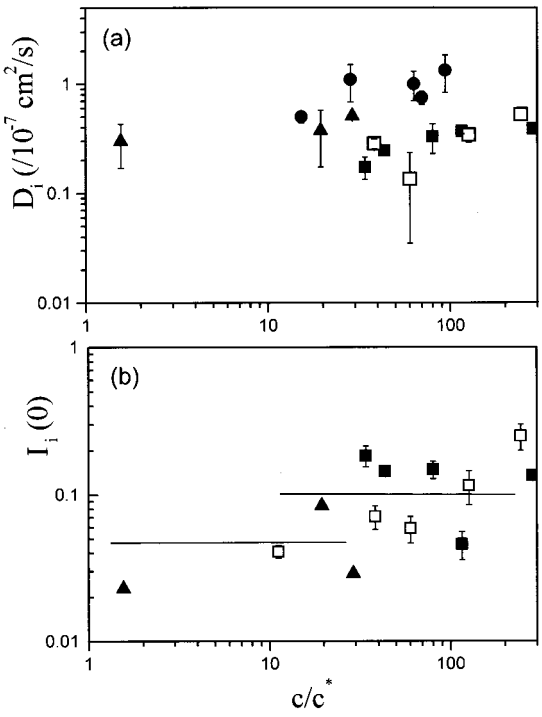

Figure 7. Diffusion coefficient D_i (a) and the intensity $I_i(0)$ (b) associated with the intermediate mode in the polarized correlation function of PPPS solutions: S1 (■), S7 (●), S9 (▲) in toluene, and of the equimolar mixture of S1 and S9 (□).

Figure 2b depicts the speed-up of D_c, above c^* due to increasing intermolecular interaction and excluded volume effects encompassed in eq 4. For semistiff chains, sizes of length $2l$ move in a more correlated fashion compared to flexible chains in semidilute solutions with smaller correlation length of the order of the blob size; the c-dependence of the latter is responsible for the scaling $D_c \propto (c/c^*)^{0.77}$ in good solvents. For concentrations between $5c^*$ and $200c^*$, the reduced D_c data in Figure 2b show a scaling exponent ≈0.9. The deviations observed at the higher concentrations ($c > 100c^*$), where the slope of the cooperative diffusion with c is smaller (especially for the higher molecular weight S1), reflect the domination of the friction effects in this concentrated regime.

C. Intermediate Diffusive Process. As already mentioned in the Experimental Section, the polarized intensity correlation functions (Figure 1) display a slow diffusive process (see below) in addition to the main fast cooperative diffusion. In the intermediate time scale, a third relaxation process contributes to the experimental $C(q,t)$ in the nondilute solutions of PPPS. Figure 6 visualizes the situation for two concentrations of S1 in toluene for which the contribution of the slow process is weak. At relatively low concentrations, e.g., 13.3% ($c/c^* = 283$), the rate of the intermediate process obtained from the second peak of the distribution $L(\ln \tau)$, is found to be diffusive (inset in Figure 6a). At higher concentrations, the depolarized intensity becomes important and its dynamics fall into the time regime of the intermediate mode; recall the VH contribution ($^4/_3 I_{VH}$) to the VV scattering.[11] In this case, the analysis of the intermediate process is obscured, and the pure diffusive character of its rate is clearly affected by the VH process, as shown in Figure 6b for a $c = 38.6\%$ ($c/c^* = 821$) solution. Due to this ambiguity in the analysis, the high concentration regime will be excluded in the discussion of the diffusive rate and the intensity of this new isotropic process.

The molecular weight polydispersity of the PPPS samples might be an obvious reason for the observation of the intermediate process. In such case, the polydispersity-induced contrast would allow the probing of composition fluctuations relaxing via self-diffusion. This mechanism has been identified in several systems including colloidal spheres,[35] rods,[8] diblock copolymers,[36] and more recently multiform star polymers;[37] the characteristic diffusion decreases while the intensity, in all but the case of multiarm stars, increases with c. To examine this possibility, we have measured the intermediate mode in a equimolar mixture of the largest (S1) with the smaller (S9) species in toluene solution. In disagreement with self-diffusion mechanism, no intensity enhancement was observed as shown by the comparison of the I_i data in Figure 7. A pertinent finding in this figure is the observation that D_I does not decrease with concentration, as expected from the increase of the self-friction, f_s, in Figure 5; instead, D_I slightly increases with concentration. Moreover, the insensitivity, within experimental error, of the intensity I_i to the c variation makes the association of the intermediate process to the self-diffusion very unlike. Instead, the former resembles the behavior of the fast cooperative diffusion.

In a two-component rigid rod/solvent system, DSO theory[9] predicts a bimodal relaxation for the concentration fluctuations as the nematic transition is approached from the isotropic state (see section II). In this model,

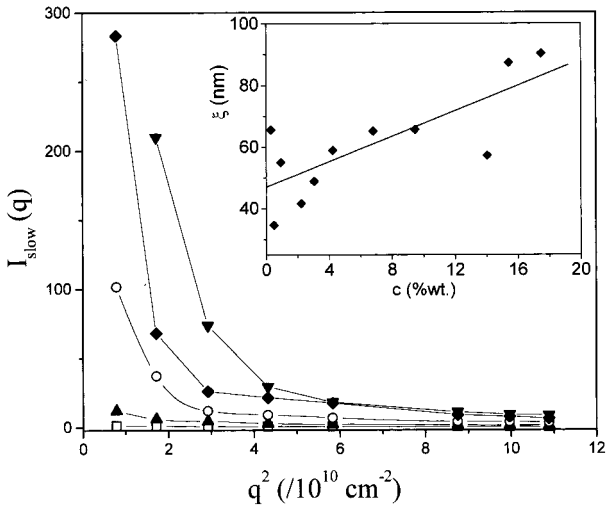

Figure 8. Variation of the intensity associated with the slow process in the dynamic polarized scattering from S3/chloroform solutions with wavevector q at different concentrations: 0.5 wt % (□), 2.2 wt % (▲), 4.2 wt % (○), 9.4 wt % (◆), 15.4 wt % (▼). The correlation length ξ obtained from the fit of Debye−Bueche relation to the intensity data is given in the inset as a function of S3 concentration.

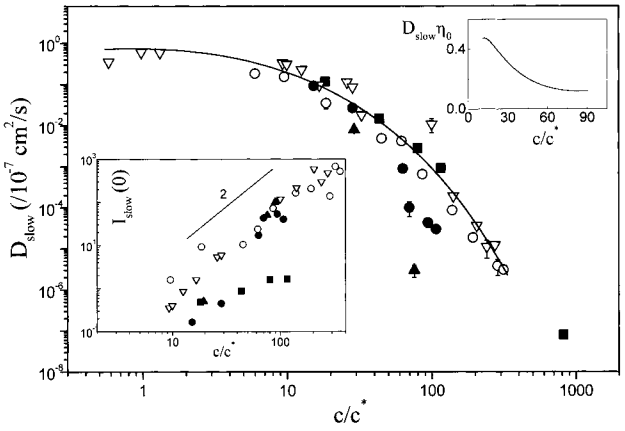

Figure 9. Variation of the slow diffusion coefficient and the associated intensity (lower inset) with the reduced concentration for four PPPS samples: S1 (■), S7 (●), S9 (▲) in toluene, S3 in chloroform (○) and TCE (▽). The concentration dependence of $D_{slow}\eta_0$ (η_0 is the zero-shear solution viscosity from Figure 9 of part 1) for S7 sample is shown in the upper inset.

the fast cooperative process dominates over the slow one as the concentration increases toward the nematic transition. The slow diffusion is associated with the relaxation of the total concentration fluctuations in the isotropic regime through both translational and rotational motions of the rods, while the fast diffusion proceeds predominantly through axial diffusion without changing the orientation of the rods. In the present case, however, it is the slow diffusion and not the fast cooperative diffusion that appears at nondilute solutions of PPPS, which noticeably do not exhibit a mesophase assumed by the DSO model.[9] Nevertheless, we can speculate on the origin of the intermediate diffusion process in the isotropic scattering based on the preferred distance in the orientation fluctuations (see also part 1[1]). These orientationally correlated pairs can affect the cooperative diffusion as additional (slower) chain displacements are probably necessary to relax fully the thermal concentration fluctuations in the hairy-rod solutions.

D. Slow Diffusion in Hairy-Rod Solutions. Albeit the PPPS samples are very soluble up to high concentrations, a slow process is present in the semidilute and concentrated regimes. As already mentioned in section II above, the intensity of the slow diffusive process is the lowest in toluene and highest in TCE increasing with c above c^* in all three solvents. This cluster-like mode in the polarized scattering represents the diffusive translational motion of a group of molecules with different refractive index from the rest of the polymer solution. For all PPPS samples but the shortest S10 (see below), the observed clusters form optically isotropic structures, as inferred from their negligibly low anisotropic (VH) scattering. The size of the clusters can be estimated from the q-dependence of the polarized intensity of $I_{slow}(q)$ for the slow mode, shown in Figure 8 for different concentrations in chloroform at 25 °C. It was found that $I_{slow}(q)$ cannot be adequately described by the common Ornstein−Zernicke equation: $I_{slow}(q) = I_{slow}(0)/(1 + q^2\xi^2)$. Instead, the Debye−Bueche expression,[1,11] $I_{slow}(q) = I_{slow}(0)/(1 + q^2\xi^2)^2$, provides a satisfactory representation of the $I_{slow}(q)$ data, with a characteristic length ξ. The Debye−Bueche expression is based on the pair distribution $f(r) = \exp(-r/\xi)$ corresponding to a medium with two randomly distributed species (clusters and molecules), with sharp interfaces between each other.[1] The size ξ in the examined concentration range (0−20%) increases from about 50 to 90 nm (inset of Figure 8).

The concentration dependence of the slow diffusion D_{slow} for four PPPS samples is shown in Figure 9. The strong slowing down of D_{slow} is dominated by the significant increase of the solution viscosity η_0 with c (see Figure 9 of part 1[1] and discussion in section IV.B). For S7 toluene solutions, the quantity $D_{slow}\eta_0$ ($\approx kT/6\pi\xi$) depicted as an inset in Figure 9, reveals an increasing ξ (60 to 200 nm) with concentration, in qualitative agreement with the static $I_{slow}(q)$ (Figure 8). In conformity to this finding, the intensity $I_{slow}(0)$ clearly deviates from the linear dependence on concentration, expected from the constant ξ, as shown in the lower inset of Figure 9.

For the shortest S10, the slow diffusive process is depolarized (VH) active (Figure 2 of part 1), implying a nonspherical shape for the clusters with finite optical anisotropy. Assuming a wormlike shape created mainly by an end-to-end association of the rodlike S10, the values of the rotational diffusion D_R ($=(1/6)\Gamma_{VH,q\to 0}$) and D_{slow} at very dilute concentrations allow the estimation of the average dimensions. Using $l = 25$ nm, eq 4, and Hearst−Stockmayer expression for the rotational diffusion coefficient of semistiff chains[27] leads to a contour length of 580 nm and diameter of 5.5 nm. The tendency for an end-to-end aggregation in S10 compared to the spherical isotropic clusters of the other PPPS is probably due to the larger chain-ends concentration and reduced solubility (low chain flexibility) for the former. The average size of the cluster is rather constant, as inferred from the linear increase of the depolarized light scattering intensity I_{VH} with c (inset in Figure 10) unlike the situation in the other PPPSs (see Figure 9). Owing probably to their wormlike shape, D_R for the dominant aggregates in S10 exhibits a concentration dependence close to the theoretical predictions for rodlike and wormlike chains (see part 1[1]), as shown in Figure 10. Similar behavior was observed for different poly(*p*-

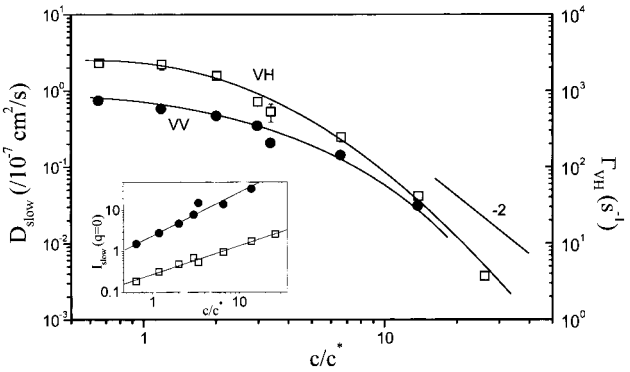

Figure 10. Concentration dependence of the diffusion coefficient D_{slow} (●) and the orientation relaxation rate Γ_{VH} (□) for the slow process in S10 toluene solutions. The intensities associated with these processes are shown in the inset.

phenylene) systems representing associates of anisotropic shapes.

V. Concluding Remarks

In this work we employed photon correlation spectroscopy in the polarized geometry in order to systematically investigate of model hairy-rod substituted poly(*p*-phenylenes) in solution and at very high concentrations (up to about 60%). The main findings of these studies can be summarized as follows:

(i) The total concentration fluctuations were found to exhibit a two-step decay. The fast relaxation process was the dominant one and was actually the "classical" cooperative diffusion found in other semiflexible polymers.[3] This process was controlled by the osmotic pressure of the system described by scaling particle theory (eq 7) for wormlike spherocylinders. On the other hand, the second relaxation process was also diffusive, but it was not related to self-diffusion (as confirmed by independent PFG-NMR measurements) and could not be accounted for by any of the existing theories.

(ii) The self-friction coefficient, f_s, was found to exhibit a very strong concentration dependence, with a slope more than two times that of the cooperative friction coefficient, f_c; thus, the behavior of f_s was clearly different from f_c. This finding clearly contradicts the assumptions of similar friction coefficients, used in the various studies for rodlike and wormlike polymers.

(iii) At high concentrations, a diffusive cluster mode was detected, despite the high solubility of these polymers in the three different solvents. The characteristics of this mode were found to depend strongly on the solvent and the molecular weight; clusters resulting from large chains (closer to flexible behavior) were isotropic, whereas those from the short ones (closer to rodlike behavior) were anisotropic.

Acknowledgment. Part of this research was supported by the Greek General Secretariat for Research and Technology (Basic Research Program, PENED-40).

References and Notes

(1) Petekidis, G.; Vlassopoulos, D.; Fytas, G.; Rulkens, R.; Wegner, G. *Macromolecules* **1998**, *31*, 6129.
(2) Petekidis, G.; Fytas, G.; Witteler, H. *Colloid Polym. Sci.* **1994**, *272*, 1457.
(3) Petekidis, G.; Vlassopoulos, D.; Fytas, G.; Fleischer, G. *Macromolecules* **1998,** 31, 1406. Petekidis, G.; Vlassopoulos, D.; Fytas, G.; Kountourakis, N.; Kumar, S. *Macromolecules* **1997**, *30*, 919.
(4) Zero, K.; Pecora, R. *Macromolecules* **1982**, *15*, 87. Tracy, M. A.; Pecora, R. *Annu. Rev. Phys. Chem.* **1992**, *43*, 525.
(5) DeLong, L. M.; Russo, P. S. *Macromolecules* **1991**, *24*, 6139. Russo, P. S. In *Dynamic Light Scattering: The Technique and Some Applications*; Oxford Science Publications: Oxford, 1993.
(6) Keep, G. T.; Pecora, R. *Macromolecules* **1988**, *21*, 817. Statman, D.; Chu, B. *Macromolecules* **1984**, *17*, 1537. Gatzonis, Y.; Siddiquee, S. K.; van Egmond, J. W. *Macromolecules* **1997**, *30*, 7253. Siddiquee, S. K.; van Egmond, J. W. *Macromolecules* **1998**, *31*, 2661.
(7) Seils, J.; Pecora, R. *Macromolecules* **1995**, *28*, 661. Goinga, H. Tj.; Pecora, R.; *Macromolecules* **1991**, *24*, 6128. Wang, L.; Garner, M. M.; Yu, H. *Macromolecules* **1991**, *24*, 2368.
(8) Buithenius, J.; Dhont, J. K. G.; Lekkekerker, H. N. W. *Macromolecules* **1994**, *27*, 7267.
(9) Shimada, T.; Doi, M.; Okano, K. *J. Chem. Phys.* **1988**, *88*, 2815; *J. Chem. Phys.* **1988**, *88*, 4070; *J. Chem. Phys.* **1988**, *88*, 7181.
(10) Petekidis, G.; Vlassopoulos, D.; Galda, P.; Rehahn, M.; Ballauff, M. *Macromolecules* **1996**, *29*, 6832.
(11) Berne, J. B.; Pecora, R. *Dynamic Light Scattering*; Wiley-Interscience Publications: New York, 1976.
(12) Broesma, S. J. *J. Chem. Phys.* **1960**, *32*, 1626; **1981**, *74*, 6989.
(13) Tracy, M.; Pecora, R. *Annu. Rev. Phys. Chem.* **1992**, *43*, 525.
(14) Yamakawa, H.; Fujii, M. *Macromolecules* **1973**, *6*, 407.
(15) Yamakawa, H. *Modern Theory of Polymer Solutions*; Harper and Row: New York, 1971. DeGennes, P. G. *Scaling Concepts in Polymer Physics*; Cornell University Press: New York, 1979.
(16) Doi, M.; Edwards, S. F. *The Theory of Polymer Dynamics*; Oxford University Press: New York, 1986.
(17) Edwards, S. F.; Evans, K. E. *Trans. Faraday Soc.* **1982**, *78*, 113.
(18) Teraoka, I.; Hayakawa, R. J. *J. Chem. Phys.* **1988**, *89*, 1988.
(19) Sato, T.; Teramoto, A. *Macromolecules* **1991**, *24*, 193.
(20) Doi, M. *J. Polym. Sci. Polym. Symp.* **1985**, *73*, 93. Odijk, T. *Macromolecules* **1984**, *17*, 502. Semenov, A. N. *J. Chem. Phys.* **1986**, *82*, 317.
(21) Sato, T.; Teramoto, A. *Adv. Polym. Sci.* **1996**, *126*, 85. Sato, T.; Takada, Y.; Teramoto, A. *Macromolecules* **1991**, *24*, 6220; **1991**, *24*, 6262.
(22) Maeda, T. *Macromolecules* **1989**, *22*, 1881; **1990**, *23*, 1464.
(23) Callaghan, P. T. *Principles of Nuclear Magnetic Resonance Microscopy*; Clarendon Press: Oxford, U.K., 1992.
(24) Vanhee, S.; Rulkens, R.; Lehmann, U.; Rosenauer, C.; Schulze, M.; Kohler, W.; Wegner, G. *Macromolecules* **1996**, *29*, 5136.
(25) Tiesler, U.; Rehahn, M.; Ballauff, M.; Petekidis, G.; Vlassopoulos, D.; Maret, G.; Kramer, H. *Macromolecules* **1996**, *21*, 6832.
(26) Kubota, K.; Chu, B. *Biopoymers* **1983**, *22*, 1461. Kubota, K.; Tominaga, Y.; Fujime, S. *Macromolecules* **1986**, *19*, 1604. Tinland, B.; Maret, G.; Rinaudo, M. *Macromolecules* **1990**, *23*, 596.
(27) Hearst, J. E.; Stockmayer, W. H. *J. Chem. Phys.* **1962**, *7*, 1425.
(28) Jinbo, Y.; Sato, T.; Teramoto, A. *Macromolecules* **1994**, *27*, 6080. Richtering, W.; Gleim, W.; Burchard, W. *Macromolecules* **1992**, *25*, 3795.
(29) Wiltzius, P.; Haller, H. R.; Canell, D. S.; Schaefer, D. W. *Phys. Rev. Lett.* **1983**, *51*, 1183.
(30) Ohta, T.; Oono, Y. *Phys. Lett.* **1982**, *89A*, 460.
(31) Coviello, T.; Burchard, W.; Dentini, M.; Crescenzi, V. *Macromolecules* **1987**, *20*, 1102.
(32) Mustafa, M. B.; Tipton, D. L.; Russo, P. S.; Barkley, M. D.; Blum, F. B. *Macromolecules* **1993**, *26*, 370.
(33) Tinland, B.; Maret, G.; Rinaudo, M. *Macromolecules* **1990**, *26*, 596.
(34) Bu, Z.; Russo, P. S.; Tipton, D. L.; Negulescu, I. I. *Macromolecules* **1994**, *27*, 6871.
(35) Pusey, P. N.; Tough R. J. A. In *Dynamic light Scattering*; Pecora, R., Ed.; Plenum Press: New York, 1985.
(36) Jian, T.; Anastasiadis, S. H.; Semenov, A. N.; Fytas, G.; Fleischer, G.; Vilesov, A. D. *Macromolecules* **1995**, *28*, 2439.
(37) Segrouchni, R.; Petekidis, G.; Vlassopoulos, D.; Fytas, G.; Semenov, A. N.; Roovers, J.; Fleischer, G. *Europhys. Lett.* **1998**, 42, 271.

MA980451S